# Conformation-dependent surface-enhanced Raman scattering of graphene oxide/metal nanoparticle hybrids

**Zhiming Liu (刘智明), Huiqing Zhong (钟会清), Zhouyi Guo (郭周义)*, and Biwen Yang (杨必文)**

*MOE Key Laboratory of Laser Life Science and SATCM Third Grade Laboratory of Chinese Medicine and Photonics Technology, College of Biophotonics, South China Normal University, Guangzhou 510631, China*

**Corresponding author: ann@scnu.edu.cn*

Received March 5, 2013; accepted June 8, 2013; posted online, 2013

Graphene oxide (GO)/Ag nanoparticle (NP) hybrids are obtained by *in situ* reduction of Ag NPs on GO sheets. In this letter, the influence of the conformation of GO sheets on the surface-enhanced Raman scattering (SERS) effect of GO/Ag NPs is investigated by covalently grafting folic acid (FA) molecules onto graphite sheets. SERS measurements are conducted in aqueous solutions with different pH values. Data show that the SERS signals of FA are pH dependent, consistent with the morphological changes of GO sheets.

*OCIS codes:* 300.6450, 160.4236.
*doi: 10.3788/COL201311.083001.*

Graphene oxide (GO) is a novel, one-atom-thick, two-dimensional carbon network containing carboxylic acid groups at the sheet edges, as well as hydroxyl and epoxy groups on the graphite plane. GO is receiving considerable attention because of its excellent physical and chemical properties, as well as potential applications in energy, electronics, sensors, and biomedicine[1−4]. GO has recently become a promising support for anchoring and dispersing various metal and metal oxide nanoparticles (NPs), such as Pt, Pd, Ag, Au, and $Fe_3O_4$[5−8]. Among the many exciting applications of GO, the use of GO/NP composites as efficient and ultrasensitive surface-enhanced Raman scattering (SERS) substrates is particularly interesting. SERS-active metal (Au or Ag) NPs have been successfully assembled onto GO sheets by *in situ* chemical reduction or electrostatic adsorption[9−12]. GO/metal NP hybrids exhibit ultrahigh SERS activity, in which GO serves as a template to enrich target molecules, thereby enhancing the presence of analytes around metal NPs[9].

GO can be well-dispersed in an aqueous solution because of the negatively charged oxygen-containing functional groups on graphene sheet[13]. Whitby *et al.*[14] have demonstrated that the morphology of GO sheets dramatically changes depending on the pH of a solution, which can be attributed to the ionization of O groups under various ionic environments. At low pH values, GO seems to agglomerate as flat sheets, whereas flaky structures tend to wrinkle and star-like morphologies form at higher pH values. Therefore, the SERS effect of GO/metal NP hybrids may be influenced by the conformational changes of GO sheets at different pH values.

To validate this hypothesis, a SERS study on folic acid (FA) at different pH values was carried out in the present work using GO/Ag NP composites as SERS substrates. In our previous work[15], we have illustrated that the non-covalent adsorption of aromatic molecules on GO sheets is significantly influenced by pH, eventually resulting in different GO-based SERS effects. To eliminate the SERS signals caused by the distinct depositing of molecules onto graphene sheets in the present study, FA molecules were covalently grafted onto GO.

The synthesis procedure of FA-GO/Ag NPs is shown in Fig. 1. FA-functionalized GO was first synthesized using a common amidation process[16]. FA-GO/Ag NP hybrids were then assembled using biocompatible polyvinylpyrrolidone (PVP) as reductant and stabilizer[6,11]. Figure 2 shows the characterization of as-prepared FA-GO/Ag NPs. The UV-VIS spectrum of GO shows a maximum absorption peak at 235 nm and a shoulder peak at about 300 nm (Fig. 2(a), curve A). After amidation, the peak at 235 nm disappears and a new peak at 275 nm emerges, indicating that FA is covalently attached onto GO successfully. The UV-VIS spectrum of FA-GO/Ag NPs (Fig. 2(a), curve C) displays a strong peak at 450 nm, indicating the formation of Ag NPs. Figure 2(b) demonstrates the Raman spectra of GO, FA-GO, and FA-GO/Ag NP solutions at pH 7. The two characterized Raman bands at 1 350 and 1 605 $cm^{-1}$ represent the D and G bands of GO, respectively. The Raman spectrum of FA-GO is similar to that of GO. However, the intensity ratio of the D band to G band increases (Fig. 2(b), curve B), indicating the mild reduction of GO during FA-GO synthesis. The Raman spectrum of FA-GO/Ag NPs demonstrates a completely different Raman pattern (Fig. 2(b), curve C), thereby providing an excellent spectral fingerprint of FA. The SERS signals of FA are so intense that the spectral information from GO is drawn out. This result further confirms the presence of FA in the hybrids. The two strongest Raman peaks at 1 505 and 1 590 $cm^{-1}$ are assigned to coupled phenyl ring deformations in FA molecules[17]. The absorption peak at 1 632 $cm^{-1}$ (vibration mode of CO–NH) in the FT-IR spectrum of FA-GO-PVP also proves that the FA molecules are anchored onto the GO surface (Fig. 2(c)). Transmission electron microscopy (TEM) analysis was performed to investigate the morphology of the obtained FA-GO/Ag NPs. Figure 2(d) shows that Ag NPs with irregular shapes and sizes of about 5 – 20 nm are randomly

 

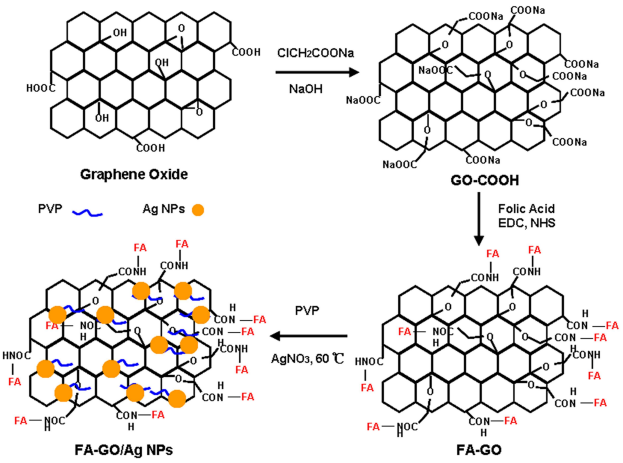


Fig. 1. Fabrication of FA-GO/Ag NPs.

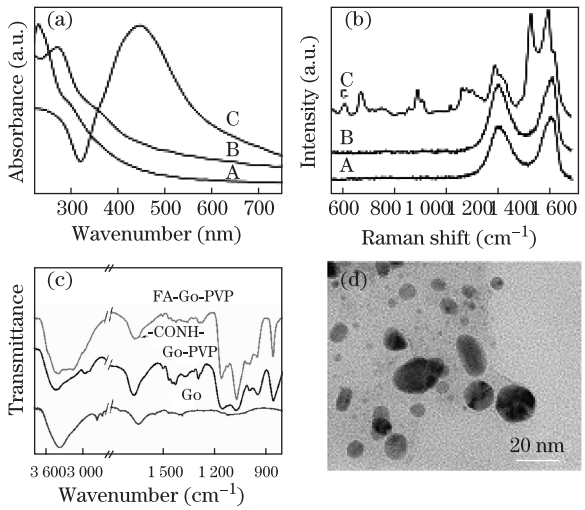


Fig. 2. (a) UV-VIS spectra and (b) Raman characterization of GO (A), FA-GO (B), and FA-GO/Ag NP (C) solutions at pH 7. (c) FT-IR spectra of GO, GO-PVP, and FA-GO-PVP. (d) TEM image of FA-GO/Ag NPs.

distributed onto the surface of graphite sheet.

In this strategy, GO acts as a bridge between FA molecules and Ag NPs; thus, strong SERS signals of FA can emerge from interstitial sites in FA-GO/Ag NPs consisting of coupled Ag NPs, namely, hotspots. The SERS response of FA-GO/Ag NPs is observed in citric acid–phosphate buffer solutions at various pH values. Raman spectra were collected with a Renishaw inVia confocal Raman spectrometer equipped with a 514.5-nm laser (0.5 mW) and an integration time of 30 s. Figure 3 describes the SERS spectra of FA (1 $\mu$mol/L) induced by Ag NPs (Fig. 3(a)) and the Raman spectra of FA-GO/Ag NPs (Fig. 3(b)) in citric acid–phosphate buffer solutions with different pH values. The SERS spectra of FA are drastically influenced by pH, indicating that the Raman scattering event on dissociative Ag NPs or on GO-Ag NPs is pH controlled. However, the two events seem to be totally different.

To further investigate the difference between Ag NP-induced SERS spectrum and the SERS spectrum generated from FA-GO/Ag NPs in response to pH, the relative intensities of the four pair of Raman peaks were plotted on Fig. 4. A Raman shift sometimes occurs in the SERS spectrum induced by Ag NPs probably because of the instability of Ag NPs in citric acid–phosphate buffer solutions. For example, the strong peak at 1 185 cm$^{-1}$ at low pH values red shifts to 1 179 cm$^{-1}$ when at pH 5. By contrast, the SERS spectral pattern of FA induced by GO/Ag NPs is stable with a negligible frequency shift. Furthermore, gradually enhanced Raman signals are observed in the FA-GO/Ag NP-induced SERS spectra. Only very weak Raman peaks are observed in the SERS spectrum at pH 3. The intensities of the four bands significantly enlarge with increased pH, especially the phenyl ring deformation mode at 1 505 cm$^{-1}$. However, no regular changes are found in the normalized intensities of the corresponding peaks induced by Ag NPs as a function of pH.

A mechanism of conformational changes of the GO sheet is proposed to explain the gradually enhanced SERS signals of FA induced by GO/Ag NPs (Fig. 5). Under acidic conditions, a few Ag NPs disperse on the flat graphene sheet, resulting in weak SERS signals of FA. The isolated Ag NPs aggregate on the wrinkled GO sheet under alkaline environments, facilitating the formation of SERS hotspots. The folded structures also allow the NPs and probes to be in close proximity, and then the strong Raman enhancement of FA emerges. To confirm the structural changes, TEM images of FA-GO/Ag NPs were acquired under acidic (pH 3) and alkaline conditions (pH 14). Figure 6 shows that the color of FA-GO/Ag NP colloids changes from straw yellow at pH 3 to brown at pH 14, consistent with previously reported color changes of GO colloids[14]. The TEM image of FA-GO/Ag NPs under an acidic condition shows a flat graphite sheet onto which irregular Ag NPs are deposited (Fig. 6(a)). However, the membranous structure

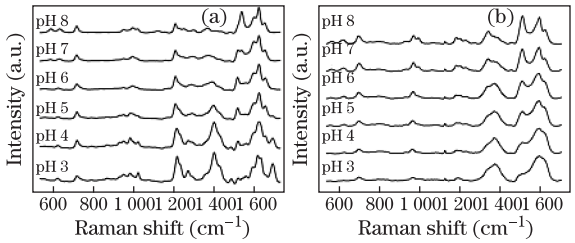


Fig. 3. (a) SERS spectra of FA (1 $\mu$M) induced by Ag NPs and (b) the Raman spectra of FA-GO/Ag NPs in citric acid–phosphate buffer solutions at different pH values normalized to the Raman band at 1590 cm$^{-1}$.

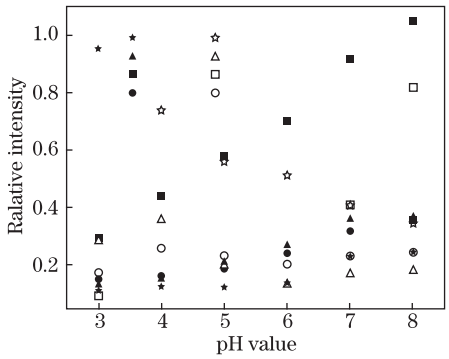


Fig. 4. Normalized intensities of some typical peaks as a function of pH.

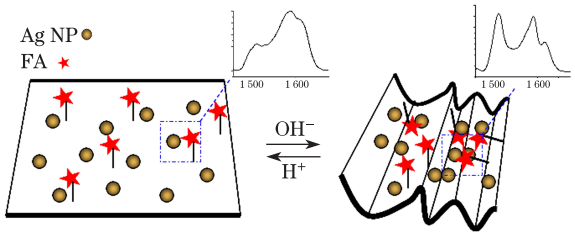


Fig. 5. Probable mechanism underlying the pH-dependent SERS effect of GO/Ag NPs.

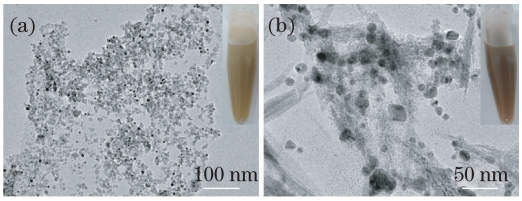


Fig. 6. TEM images of FA-GO/Ag NPs at (a) pH 3 and (b) pH 14. Insets show the corresponding photographs of FA-GO/Ag NPs colloids.

becomes folded at pH 14, which leads to the overlapping of Ag NPs on GO sheet (Fig. 6(b)). The wrinkling of FA-GO/Ag NP sheet at high pH values can facilitate the SERS event between Ag NPs and FA, thereby causing strong SERS signals (Fig. 3(b)).

In conclusion, GO/Ag NP hybrids covalently functionalized with FA are obtained by *in situ* reduction of Ag NPs on GO surface using PVP as reductant and stabilizer. The hybrids exhibit highly sensitive and reproducible pH-dependent SERS responses within pH 3.0 to 8.0, which can be attributed to the conformational changes of GO sheet.

This work was supported by the National Natural Science Foundation of China (No. 60778047), the Specialized Research Fund for the Doctoral Program of Higher Education of China (No. 20114407110001), the Natural Science Foundation of Guangdong Province (No. 9251063101000009), and the Cooperation Project in Industry, Education, and Research of Guangdong Province and Ministry of Education of China (No. 2011A090200011).

## References

1. V. Georgakilas, M. Otyepka, A. B. Bourlinos, V. Chandra, N. Kim, K. C. Kemp, P. Hobza, R. Zboril, and K. S. Kim, Chem. Rev. **112,** 6156 (2012).
2. Y. K. Yap, R. M. D. L. Rue, C. H. Pua, S. W. Harun, and H. Ahmad, Chin. Opt. Lett. **10,** 041405 (2012).
3. W. Zhang, Z. Guo, D. Huang, Z. Liu, X. Guo, and H. Zhong, Biomaterials **32,** 8555 (2011).
4. Y. Fan, Z. Jiang, and L. Yao, Chin. Opt. Lett. **10,** 071901 (2012).
5. S. Guo, S. Dong, and E. Wang, ACS Nano **4,** 547 (2009).
6. X. Z. Tang, Z. W. Cao, H. B. Zhang, J. Liu, and Z. Z. Yu, Chem. Commun. **47,** 3084 (2011).
7. Z. Liu, C. Hu, S. Li, W. Zhang, and Z. Guo, Anal. Chem. **84,** 10338 (2012).
8. W. Chen, P. Yi, Y. Zhang, L. Zhang, Z. Deng, and Z. Zhang, ACS Appl. Mater. Interfaces **3,** 4085 (2011).
9. W. Ren, Y. Fang, and E. Wang, ACS Nano **5,** 6425 (2011).
10. Z. Liu, Z. Guo, H. Zhong, X. Qin, M. Wan, and B. Yang, Phys. Chem. Chem. Phys. **15,** 2961 (2013).
11. Z. Zhang, F. Xu, W. Yang, M. Guo, X. Wang, B. Zhang, and J. Tang, Chem. Commun. **47,** 6440 (2011).
12. J. Huang, L. Zhang, B. Chen, N. Ji, F. Chen, Y. Zhang, and Z. Zhang, Nanoscale **2,** 2733 (2010).
13. D. Li, M. B. Muller, S. Gilje, R. B. Kaner, and G. G. Wallace, Nat. Nanotechnol. **3,** 101 (2008).
14. R. L. D. Whitby, A. Korobeinyk, V. M. Gun'ko, R. Busquets, A. B. Cundy, K. Laszlo, J. Skubiszewska-Zieba, R. Leboda, E. Tombacz, I. Y. Toth, K. Kovacs, and S. V. Mikhalovsky, Chem. Commun. **47,** 9645 (2011).
15. Z. Liu, S. Li, C. Hu, W. Zhang, H. Zhong, and Z. Guo, J. Raman Spectrosc. **44,** 75 (2013).
16. L. Zhang, J. Xia, Q. Zhao, L. Liu, and Z. Zhang, Small **6,** 537 (2010).
17. R. J. Stokes, E. McBride, C. G. Wilson, J. M. Girkin, W. E. Smith, and D. Graham, Appl. Spectrosc. **62,** 371 (2008).